ELSEVIER

PII: S0032-3861(97)00615-0

Polymer Vol. 39 No. 13, pp. 2951–2961, 1998

0032-3861/98/$19.00+0.00

Synthesis and characterization of side-chain liquid-crystalline poly(ether carbonate)s containing biphenyl-based mesogenic groups

Ben-Ruey Liaw* and Ming-An Li

Graduate School of Chemical Engineering, National Taiwan University of Science and Technology, 43 Keelung Road, Section 4, Taipei 106, Taiwan, Republic of China
(Received 7 April 1997; revised 26 May 1997; accepted 22 July 1997)

A homologous series of new spiro-orthocarbonate monomers **4**, containing biphenyl mesogens at C-3 and C-9 positions of the six-membered spirocyclic ring through the alkylene spacers of different lengths, were prepared by condensation reaction of the corresponding biphenyl mesogenic 1,3-propanediol **3** with tetramethyl orthocarbonate. By opening of the spirocyclic ring with boron trifluoride etherate, spiro-orthocarbonate monomers **4** afforded a novel class of side-chain thermotropic LC polymer with poly(ether carbonate) as the main chain **6**. Comparison of the thermal transitions of polymers **6** with those of the corresponding monomers **4** showed that the monomers exhibit far higher isotropic temperatures than the polymers. The ability of the tail groups (NO_2, F, BuO and CN) to stabilize the mesophases in side-chain liquid-crystalline poly(ether carbonate)s closely parallels the effect of the tails for spiro-orthocarbonate monomers.

(Keywords: poly(ether carbonate); cationic ring-opening polymerization; side-chain liquid-crystalline polymers)

INTRODUCTION

Design and synthesis of side-chain or comb-like liquid-crystalline polymers containing mesogenic groups attached through a flexible spacer to the central polymer backbone attract great interest, since these polymers are regarded as materials with promising optical and electro-optical properties for potential applications in optical switching and image storage[1]. Since the first report on the application of cationic ring polymerization of cyclic iminoethers possessing biphenyl mesogenic groups for preparation of side-chain liquid-crystalline poly(*N*-acylethyleneimine)s by Percec[2] in 1987, the ring-opening polymerization (ROP) of lactones[3], epoxides[4], thiranes[5], oxetanes[6–8] and 1-methyl-1-silacyclopent-3-enes[9] containing mesogenic groups has been developed extensively. More recently, ring-opening metathesis polymerization[10] (ROMP) has also been used to polymerize norbornene containing a variety of mesogenic groups with different spacer lengths to give norbornene-based side-chain liquid-crystalline polymers with well-defined structures.

This paper reports the results of studies on preparation of liquid-crystalline poly(ether carbonate)s **6** by cationic ring-opening polymerization (ROP) of the corresponding mesogenic spiro-orthocarbonate monomers **4**. The thermal behaviour of the resulting polymers is also studied by differential scanning calorimetry (d.s.c.) and optical polarized microscopy (OPM) to elucidate their liquid-crystalline properties.

EXPERIMENTAL

Techniques

^1H and ^{13}C n.m.r. spectra were recorded on JEOL EX-400 MHz and Bruker AW-300WB *FT*n.m.r. spectrometers. *FT*i.r. spectra were recorded on a JASCO FT/IR-700. Mass spectra were obtained from a Finnigan MAT TSQ-46C g.c.–m.c.s.–m.s.–d.s. spectrometer operated at an ionizing potential of 70 eV. High-resolution mass spectra (h.r.m.s.) were obtained with a JEOL JMS 110 mass spectrometer.

A Mettler TCII, TA-4000 differential scanning calorimeter, equipped with Graph Ware TA 72.2/5, was used to determine the thermal transitions, which were read at the maximum of their endothermic or exothermic peaks. In all cases, the heating and cooling rates were 10°C min^{-1}, unless otherwise specified. The midpoint of the change in heat capacity was considered as the glass transition temperature (T_g). After the first heating scan, the samples were annealed at ~10°C above the isotropization temperature for 5 min. The transitions reported were read during the first cooling and second heating scans, unless otherwise specified. A Nikon AFX-DX optical microscope (magnification 200 ×), equipped with a Mettler FP 82 hot stage and a Mettler FP 90 central processor, was used to observe the thermal transitions and to analyse the anisotropic textures.

Molecular weight and its distribution (MWD: M_w/M_n) were determined with an h.p.l.c. JASCO 880-PU system, equipped with two polystyrene columns (Ultrastyragel, particle size 5 μm, pore size mixed D), using THF as an eluent, at a flow rate of 1.0 mL min^{-1}, polystyrene calibration, and a PL-EMD950 solvent evaporized mass detector (Polymer Laboratories Ltd).

Materials

Solvents and reagents were used after proper drying and purification. 4-Hydroxy-4′-fluorobiphenyl was prepared from 4-hydroxy-4′-nitrobiphenyl[11] following the published procedure[12]. 4-Butoxy-4′-hydroxybiphenyl was prepared by the reported procedure[13].

* To whom correspondence should be addressed

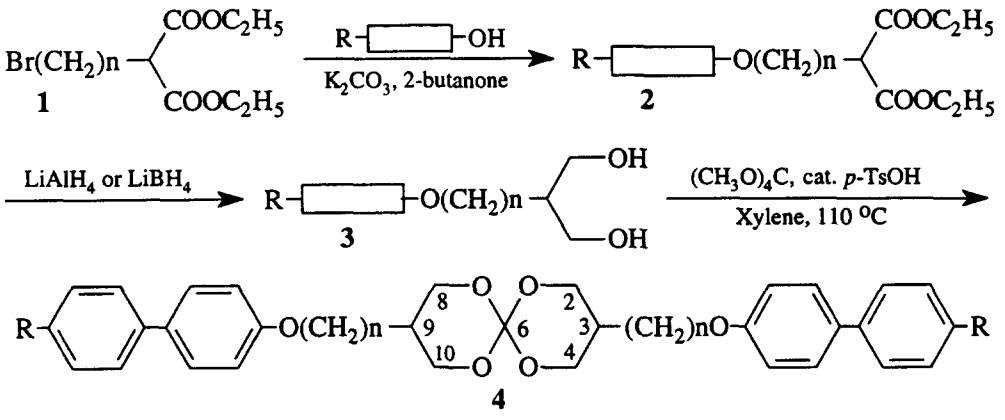

MnNO2: R = NO2 (n = 2~10); MnBuO: R = BuO (n = 6, 10);
MnCN: R = CN (n = 6, 10), and MnF: R = F (n = 6, 10).

Scheme 1 Synthesis of spiro-orthocarbonate monomers having *p*-substituted biphenyl mesogenic groups (M*n*NO$_2$, M*n*BuO, M*n*CN and M*n*F), **4**

Spiro-orthocarbonate monomers **4** containing biphenyl-based mesogens attached by spacer groups of different lengths were prepared according to the route shown in *Scheme 1*.

General procedure for preparation of p-substituted biphenyl mesogenic diethyl malonates 2 (R = NO$_2$, n = 2–10; R = CN, n = 6,10; R = BuO, n = 6,10; R = F, n = 6,10)

All *p*-substituted biphenyl mesogenic diethyl malonates **2** were prepared by the experimental procedure used for diethyl 2-[8-(4′-nitro-4-hydroxybiphenyloxy)octyl] malonate **2** (R = NO$_2$, *n* = 8), which is reported in detail as a typical example.

A suspension of 4-nitro-4′-hydroxybiphenyl (12.0 g, 0.06 mol), potassium carbonate (10.37 g, 0.08 mol), diethyl-2-(8-bromohexyl) malonate **1** (22.9 g, 0.07 mol), and 18-crown-6-ether (15 mg) in 2-butanone (300 mL) was heated to reflux for 24 h[14]. After cooling and filtration, the solvent was distilled off and the product was purified by column chromatography (silica gel, EAc–hexane = 1:4 eluent) to yield *diethyl 2-[8-(4′-nitro-4-hydroxybiphenyloxy) octyl] malonate 2* (R = NO$_2$, *n* = 8), a pale yellow liquid, with 79.8% yield. M.s.: *m/z* (rel.%): 485 (M$^+$, 36%); 215 (100%). ^{1}H n.m.r. (CDCl$_3$, ppm): 1.27 (t, 6H, *J* = 7.10 Hz, CH$_3$); 1.34–1.89 (m, 14H, (CH$_2$)$_7$CH); 3.33 (t, 1H, *J* = 7.58 Hz, CH); 3.99 (t, 2H, *J* = 6.58 Hz, biphenyl–OCH$_2$); 4.17–4.22 (m, 4H, OCH$_2$CH$_3$); 6.97–8.23 (m, 8H, biphenyl protons).

Diethyl 2-[6-(4′-cyano-4-biphenyloxy)hexyl] malonate 2 (R = CN, *n* = 6), a white solid, with 67.0% yield. M.s.: *m/z* (rel.%) 437 (M$^+$, 40%); 195 (100%). ^{1}H n.m.r. (CDCl$_3$, ppm): 1.40–1.94 (m, 10H, (CH$_2$)$_5$CH); 4.17–4.22 (m, 4H, OCH$_2$CH$_3$); 6.97–7.69 (m, 8H, biphenyl protons).

Diethyl 2-[6-(4′-fluoro-4-biphenyloxy)decyl] malonate 2 (R = F, *n* = 6), a white solid, with 76.2% yield. M.s.: *m/z* (rel.%): 430 (M$^+$, 39%); 188 (100%). ^{1}H n.m.r. (CDCl$_3$, ppm): 3.97 (t, 2H, *J* = 6.36 Hz, biphenyl–OCH$_2$); 6.93–7.50 (m, 8H, biphenyl protons).

Diethyl 2-[6-(4′-biphenyloxy)decyl] malonate 2 (R = BuO, *n* = 6), a white solid, with 69.6% yield. M.s.: m/z (rel. %): 484 (M$^+$, 43%); 234 (100%). ^{1}H n.m.r. (CDCl$_3$, ppm): 0.98 (t, 3H, *J* = 7.32 Hz, CH$_3$); 1.37–1.94 (m, 14H, (CH$_2$)$_2$CH and OCH$_2$(CH$_2$)$_5$); 3.94–4.00 (m, 4H, CH$_2$-biphenyl–OCH$_2$); 6.91–7.46 (m, 8H, biphenyl protons). Other protons were observed at reasonable positions.

General procedure for preparation of p-substituted biphenyl mesogenic propane-1,3-diols 3 (R = NO$_2$, n = 2–10; R = CN, n = 6,10)

All *p*-substituted biphenyl mesogenic propane-1,3-diols **3** were prepared by the reduction of lithium borohydride (3-molar to the ester) in THF at 0°C. After usual workup, the crude product from **2** (R = NO$_2$, *n* = 8) was flash-chromatographed on silica gel with dichloromethane–ethylacetate (1:1) to yield *2-[8-(4′-nitro-4-biphenyloxy) hexyl]propane-1,3-diol 3* (R = NO$_2$, *n* = 8), a yellow-brown solid, m.p.: 57.5–59.0°C, in yield 75.0%. M.s.: *m/z* (rel.%): 401 (M$^+$, 51%); 215 (100%). ^{1}H n.m.r. (CDCl$_3$, ppm): 1.23–1.46 (m, 12H, OCH$_2$CH$_2$(CH$_2$)$_6$CH); 1.27 (m, 4H, O(CH$_2$)$_2$CH$_2$CH$_2$CH$_2$); 1.38 (m, 2H, CH$_2$CH); 1.76–1.83 (m, 3H, Ar–OCH$_2$CH$_2$ and CH); 2.59 (s, 2H, OH); 3.64 (t, 2H, *J* = 7.80 Hz, CHH′OH); 3.81 (dd, 2H, *J* = 10.50, 3.66 Hz, CHH′OH); 4.00 (t, 2H, *J* = 6.60 Hz, biphenyl–OCH$_2$); 6.98–8.25 (m, 8H, *J* = 8.78 Hz, biphenyl protons).

2-[6-(4′-Cyano-4-biphenyloxy)hexyl]propane-1,3-diol 3 (R = CN, *n* = 6), a white solid, m.p.: 109.5–110.3°C, with 80.9% yield. M.s.: *m/z* (rel.%): 353 (M$^+$, 49%); 195 (100%). ^{1}H n.m.r. (CDCl$_3$, ppm): 1.27 (m, 2H, O(CH$_2$)$_3$CH$_2$); 1.36–1.40 (m, 4H, O(CH$_2$)$_2$CH$_2$CH$_2$CH$_2$); 1.48 (m, 2H, CH$_2$CH); 1.98 (s, 2H, OH); 3.67 (dd, 2H, *J* = 10.47, 7.34 Hz, CHH′OH); 6.97–7.70 (m, 8H, biphenyl protons).

Other p-substituted biphenyl mesogenic propane-1,3-diols 3 (R = BuO, *n* = 6,10; R = F, *n* = 6,10) were similarly synthesized using lithium aluminum hydride.

2-[6-(4′-Fluoro-4-biphenyloxy)decyl]propane-1,3-diol 3 (R = F, *n* = 6), a white solid, m.p.: 110.4–111.0°C, with 83.7% yield. M.s.: *m/z* (rel.%): 346 (M$^+$, 55%); 188 (100%). ^{1}H n.m.r. (CDCl$_3$, ppm): 2.90 (s, 2H, OH); 3.60–3.69 (m, 2H, CHH′OH); 3.78–3.85 (m, 2H, CHH′OH); 3.98 (t, 2H, *J* = 6.36 Hz, biphenyl–OCH$_2$); 6.94–7.56 (m, 8H, biphenyl protons). Other protons were observed at reasonable positions.

General procedure for preparation of spiro-orthocarbonates 4 (MnNO$_2$, R = NO$_2$, n = 2–10; MnCN, R = CN, n = 6,10; MnBuO, R = BuO, n = 6,10; MnF, R = F, n = 6,10)

Monomers (M*n*NO$_2$, M*n*CN, M*n*BuO and M*n*F) were prepared by the ester exchange reaction of tetramethyl orthocarbonate with **3** in the presence of *p*-toluenesulfonic

acid in xylene at 110°C. Triethylamine (0.01 mL) was added after cooling under nitrogen. The solution was allowed to stand overnight at room temperature and the crystalline solid formed was filtered off and washed with acetone. The product was recrystallized twice from ethyl acetate to give 1.50 g (47.0%) of yellow crystals of *3,9-bis[8-(4'-nitro-4-biphenylyloxy)octyl]-1,5,7,11-tetraoxaspiro[5.5]undecane* **4**, $MnNO_2$ (R = NO_2, $n = 8$) from **3** (R = NO_2, $n = 8$).

^{1}H n.m.r. (δ, ppm, C_6D_6): 0.98–1.44 (m, 24H, $CH_2(CH_2)_6CH_2O$); 1.63–1.71 (m, 6H, H3, H9 and $CHCH_2$); 3.65 (dd, 2H, J = 10.60, 8.88 Hz, H2a and H10a); 3.74 (3.74 (m, 2H, ArO–CH_2); 3.78 (dd, 2H, J = 10.80, 8.90 Hz, H4a and H8a); 3.88 (dd, 2H, J = 9.6, 4.44 Hz, H2e and H10e); 3.94 (dd, 2H, J = 9.80, 4.44 Hz, H4e and H8e); 6.89–7.95 (m, 16H, biphenyl protons). ^{13}C n.m.r. (δ, ppm, $CDCl_3$): 26.3, 26.9, 28.5, 29.5, 29.6, 29.7 29.9 (CH_2); 33.4 (C3 and C9); 66.6 (C2 and C10); 67.0 (C4 and C8); 68.1 (ArO–CH_2); 115.3 (C6); 115.4 (Cs); 124.1 (Cu'); 127.1 (Cs'); 128.8 (Cu); 131.1 (Ct); 146.9 (Ct'); 147.0 (Cr'); 160.4 (Cr). I.r. (KBr, cm^{-1}): 1011, 1104 (s, νC–O–C); 1253 (s, νAr–O–C); 1337 (s, $\nu_s NO_2$); 1505 (s, $\nu_{as} NO_2$).

For the homologous series of other monomers **4**, only characteristic absorption peaks in ^{1}H n.m.r., ^{13}C n.m.r. and i.r. analysis data are shown here. Other aliphatic protons (or carbons), aromatic protons (or carbons) and the peaks corresponding to various C–O–C stretching models (aliphatic or aromatic ether linkage) were observed at the expected positions. The DEPT subspectrum was used for the assignment of the signals. Ha and He represent the protons at the axial and equatorial positions in the six-membered spirocyclic ring of the monomer, respectively.

3,9-Bis[2-(4'-nitro-4-biphenyloxy)ethyl]-1,5,7,11-tetraoxaspiro[5.5]undecane $MnNO_2$ (R = NO_2, $n = 2$).

^{1}H n.m.r. (δ, ppm, C_6D_6): 2.01–2.04 (m, 2H, H3 and H9); 3.72 (dd, 2H, J = 10.80, 8.80 Hz, H2a and H10a); 3.84 (dd, 2H, J = 10.85, 9.00 Hz, H4a and H8a); 4.00–4.06 (m, 6H, H2e, H8e and ArO–CH_2); 4.07 (dd, 2H, J = 9.50, 7.10 Hz, H4e and H8e). ^{13}C n.m.r. (δ, ppm, $CDCl_3$): 32.6 (C3 and C9); 66.4 (C2 and C10); 66.8 (C4 and C8); 67.8 (ArO–CH_2); 114.6 (C6). I.r. (KBr, cm^{-1}): 1342 (s, $\nu_s NO_2$); 1503 (s, $\nu_{as} NO_2$).

3,9-Bis[3-(4'-nitro-4-biphenyloxy)propyl]-1,5,7,11-tetraoxaspiro[5.5]undecane $MnNO_2$ (R = NO_2, $n = 3$).

^{1}H n.m.r. (δ, ppm, $CDCl_3$): 2.02–2.05 (m, 2H, H3 and H9); 3.74 (dd, 2H, J = 10.84, 8.84 Hz, H2a and H10a); 3.86 (dd, 2H, J = 10.87, 9.07 Hz, H4a and H8a); 4.00–4.05 (m, 6H, H2e, H8e and ArO–CH_2); 4.09 (dd, 2H, J = 9.48, 7.20 Hz, H4e and H8e). ^{13}C n.m.r. (δ, ppm, $CDCl_3$): 32.7 (C3 and C9); 66.4 (C2 and C10); 66.8 (C4 and C8); 67.8 (ArO–CH_2); 114.5 (C6). I.r. (KBr, cm^{-1}): 1340 (s, $\nu_s NO_2$); 1504 (s, $\nu_{as} NO_2$).

3,9-Bis[4-(4'-nitro-4-biphenyloxy)butyl]-1,5,7,11-tetraoxaspiro[5.5]undecane $MnNO_2$ (R = NO_2, $n = 4$).

^{1}H n.m.r. (δ, ppm, C_6D_6): 1.67–1.68 (m, 2H, H3 and H9); 3.59 (m, 4H, ArO–CH_2); 3.64 (dd, 2H, J = 10.62, 8.56 Hz, H2a and H10a); 3.78 (dd, 2H, J = 10.84, 8.52 Hz, H4a and H8a); 3.88 (dd, 2H, J = 6.36, 4.16 Hz, H2e and H8e); 3.95 (dd, 2H, J = 6.32, 4.48 Hz, H4e and H8e). ^{13}C n.m.r. (δ, ppm, $CDCl_3$): 33.3 (C3 and C9); 66.4 (C2 and C10); 66.7 (C4 and C8); 67.7 (ArO–CH_2); 115.20 (C6). I.r. (KBr, cm^{-1}): 1335 (s, $\nu_s NO_2$); 1514 (s, $\nu_{as} NO_2$).

3,9-Bis[5-(4'-nitro-4-biphenyloxy)pentyl]-1,5,7,11-tetraoxaspiro[5.5]undecane $MnNO_2$ (R = NO_2, $n = 5$).

^{1}H n.m.r. (δ, ppm, $CDCl_3$): 1.92–1.96 (m, 2H, H3 and H9); 3.65 (dd, 2H, J = 10.68, 9.64 Hz, H2a and H10a); 3.79 (dd, 2H, J = 10.72, 9.44 Hz, 4a and H8a); 3.91–4.02 (m, 8H, H2e, H8e, H4e, H8e and ArO–CH_2. ^{13}C n.m.r. (δ, ppm, $CDCl_3$): 32.8 (C3 and C9); 66.5 (C2 and C10); 67.0 (C4 and C8); 67.9 (ArO–CH_2); 114.5 (Co). I.r. (KBr, cm^{-1}): 1337 (s, $\nu_s NO_2$); 1511 (s, $\nu_{as} NO_2$).

3,9-Bis[6-(4'-nitro-4-biphenyloxy)hexyl]-1,5,7,11-tetraoxaspiro[5.5]undecane $MnNO_2$ (R = NO_2, $n = 6$).

^{1}H n.m.r. (δ, ppm, C_6D_6): 1.92–2.00 (m, 2H, H3 and H9); 4.65 (dd, 2H, J = 10.00, 9.28 Hz, H2a and H10a); 3.80 (dd, 2H, J = 10.08, 9.28 Hz, H4a and H8a); 3.94 (dd, 2H, J = 9.80, 4.44 Hz, H2e and H10e); 4.10–4.18 (n, 6H, ArO–CH_2 and H4e and H8e). ^{13}C n.m.r. (δ, ppm, C_6D_6: 32.7 (C3 and C9); 66.5 (C2 and C10); 67.0 (C4 and C8); 67.9 (ArO–CH_2); 114.3 (C6). I.r. (KBr, cm^{-1}): 1337 (s, $\nu_s NO_2$); 1511 (s, $\nu_{as} NO_2$).

3,9-Bis[7-(4'-nitro-4-biphenyloxy)heptyl]-1,5,7,11-tetraoxaspiro[5.5]undecane $MnNO_2$ (R = NO_2, $n = 7$).

^{1}H n.m.r. (δ, ppm, C_6D_6): 1.68–1.72 (m, 2H, H3 and H9); 3.67 (dd, 2H, J = 10.60, 8.66 Hz, H2a and H10a); 3.72 (m, 4H, ArO–CH_2); 3.78 (dd, 2H, J = 10.68, 8.90 Hz, H4a and H8a); 3.89 (dd, 2H, J = 10.70, 4.60 Hz, H2e and H10e); 3.97 (dd, 2H, J = 10.60, 4.56 Hz, H4e and H8e). ^{13}C n.m.r. (δ, ppm, C_6D_6): 33.3 (C3 and C9); 66.6 (C2 and C10); 66.9 (C4 and C8); 68.10 (ArO–CH_2); 115.30 (C6). I.r. (KBr, cm^{-1}): 1337 (s, $\nu_s NO_2$); 1513 (s, $\nu_{as} NO_2$).

3,9-Bis[9-(4'-nitro-4-biphenyloxy)nonyl]-1,5,7,11-tetraoxaspiro[5.5]undecane $MnNO_2$ (R = NO_2, $n = 9$).

^{1}H n.m.r. (δ, ppm, C_6D_6): 1.90–1.93 (m, 2H, H3 and H9); 3.62 (dd, 2H, J = 10.64, 9.84 Hz, H2a and H8a); 3.77 (dd, 2H, J = 10.76, 9.64 Hz, H4a and H8a); 3.90 (dd, 2H, J = 10.16, 3.48 Hz, H2e and H8e); 3.96–4.00 (m, 6H, ArO–CH_2 and H4e and H8e). ^{13}C n.m.r. (δ, ppm, C_6D_6): 32.9 (C3 and C9); 66.6 (C2 and C10); 67.1 (C4 and C8); 68.2 (ArO–CH_2); 115.2 (C6). I.r. (KBr, cm^{-1}): 1338 (s, $\nu_s NO_2$); 1504 (s, $\nu_{as} NO_2$).

3,9-Bis[10-(4'-nitro-4-biphenyloxy)decyl]-1,5,7,11-tetraoxaspiro[5.5]undecane $MnNO_2$ (R = NO_2, $n = 10$).

^{1}H n.m.r. (δ, ppm, $CDCl_3$): 1.85–1.96 (m, 2H, H3 and H9); 3.65 (dd, 2H, J = 10.40, 9.30 Hz, H2a and H8a); 3.78 (dd, 2H, J = 10.32, 9.50 Hz, H4a and H8a); 3.85–4.01 (m, 8H, ArO–CH_2 and H2e, H10e, H4e, H8e). ^{13}C n.m.r. (δ, ppm, $CDCl_3$): 32.9 (C3 and C9); 66.6 (C2 and C10); 67.2 (C4 and C8); 68.2 (ArO–CH_2); 115.2 (C6). I.r. (KBr, cm^{-1}): 1340 (s, $\nu_s NO_2$); 1504 (s, $\nu_{as} NO_2$).

3,9-Bis[6-(4'cyano-4-biphenyloxy)hexyl]-1,5,7,11-tetraoxaspiro[5.5]undecane MnCN (R = CN, $n = 6$).

^{1}H n.m.r. (δ, ppm, $CDCl_3$): 1.88–1.99 (m, 2H, H3 and H9); 3.63 (dd, 2H, J = 10.10, 10.64 Hz, H2a and H10a); 3.79 (dd, 2H, J = 10.14, 10.76 Hz, H4a and H8a); 3.92 (dd, 2H, J = 10.84, 4.44 Hz, H2e and H10e); 3.96–4.01 (m, 6H, ArO–CH_2 and H4e and H8e). ^{13}C n.m.r. (δ, ppm, $CDCl_3$): 32.8 (C3 and C9); 66.5 (C2 and C10); 67.0 (C4 and C8); 67.9 (ArO–CH_2); 114.4 (C6). I.r. (KBr, cm^{-1}): 2216 (s, νCN).

3,9-Bis[10-(4'-cyano-4-biphenyloxy)decyl]-1,5,7,11-tetraoxaspiro[5.5]undecane MnCN (R = CN, $n = 10$).

^{1}H n.m.r. (δ, ppm, $CDCl_3$): 1.85–1.96 (m, 2H, H3 and H9) 3.65 (dd, J = 10.40, 9.30 Hz, H2a and H10a); 3.78 (dd, 2H, J = 10.32, 9.50 Hz, H4a and H8a); 3.85–4.01 (m, 8H, H2e, H10e, H4e, H8e and ArO–CH_2). ^{13}C n.m.r. (δ, ppm, $CDCl_3$): 32.9 (C3 and C9); 66.6 (C2 and C10); 67.2 (C4 and C8); 68.2 (ArO–CH_2); 114.5 (C6). I.r. (KBr, cm^{-1}): 2216 (s, νCN).

3,9-Bis[6-(4'-fluoro-4-biphenyloxy)hexyl]-1,5,7,11-tetraoxaspiro[5.5]undecane MnF (R = F, ntsave = 6).

^{1}H n.m.r. (δ, ppm, $CDCl_3$): 1.92–1.96 (m, 2H, H3 and H9); 3.64 (dd, 2H, J = 10.14, 9.52 Hz, H2a and H10a); 3.79

(dd, 2H, J = 10.14, 9.68 Hz, H4e and H8e); 3.91–4.01 (m, 8H, H2e, H10e, H4e, H8e and ArO–CH_2). ^{13}C n.m.r. (δ, ppm, $CDCl_3$): 32.9 (3 and C9); 66.6 (C2 and C10); 67.1 (C4 and C8); 67.9 (ArO–CH_2); 114.5 (C6). I.r. (KBr, cm^{-1}): 1212 (s, νCF).

3,9-Bis[10-(4'-fluoro-4-biphenyloxy)decyl]-1,5,7,11-tetraoxaspiro[5.5]undecane MnF (R = F, n = 10).

^{1}H n.m.r. (δ, ppm, $CDCl_3$): 1.88–2.01 (m, 2H, H3 and H9); 3.65 (dd, 2H, J = 10.10, 9.30 Hz, H2a and H10a); 3.80 (dd, 2H, J = 10.18, 10.40 Hz, H2e and H10e); 3.90–4.01 (m, 8H, ArO–CH_2 and H4e and H8e). ^{13}C n.m.r. (δ, ppm, $CDCl_3$): 32.8 (C3 and C9); 66.5 (C2 and C10); 67.1 (C4 and C8); 68.0 (ArO–CH_2); 114.4 (C6). I.r. (KBr, cm^{-1}): 1213 (s, νCF).

3,9-Bis[6-(4'-butoxy-4-biphenyloxy)hexyl]-1,5,7,11-tetraoxaspiro[5.5]undecane MnBuO (R = BuO, n = 6).

^{1}H n.m.r. (δ, ppm, $CDCl_3$): 0.98 (t, J = 7.32 Hz, CH_3); 1.23–1.53 (m, 20H, CH_3CH_2 and $CH_2(CH_2)_4CH_2O$); 1.74–1.79 (m, 4H, $CHCH_2$ and $CH_3CH_2CH_2$); 1.88–1.99 (m, 2H, H3 and H9); 3.64 (dd, 2H, J = 10.04, 9.80 Hz, H2a and H10a); 3.80 (dd, 2H, J = 10.02, 9.76 Hz, H4a and H8a); 3.92–4.00 (m, 12H, H2e, H10e, H4e, H8e and ArO–CH_2). ^{13}C n.m.r. (δ, ppm, $CDCl_3$): 32.7 (C3 and C9); 66.5 (C2 and C10); 67.0 (C4 and C8); 67.9 (ArO–CH_2); 114.4 (C6). I.r. (KBr, cm^{-1}): 1212, 1242 (s, νAr–O–C)).

3,9-Bis[10-(4'-butoxy-4-biphenyloxy)decyl]-1,5,7,11-tetraoxaspiro[5.5]undecane MnBuO (R = BuO, n = 10).

^{1}H n.m.r. (δ, ppm, $CDCl_3$): 3.64 (dd, J = 10.10, 9.30 Hz, H2a and H10a); 3.79 (dd, 2H, J = 10.18, 10.40 Hz, H4a and H8a); 3.90–4.01 (m, 12H, H2e, H10e, H4e, H8e and ArO–CH_2). ^{13}C n.m.r. (δ, ppm, $CDCl_3$): 33.0 (C3 and C9); 66.6 (C2 and C10); 66.9 (C4 and C8); 68.1 (ArO–CH_2); 115.3 (C6). I.r. (KBr, cm^{-1}): 1212, 1243 (s, νAR–O–C).

General procedure for preparation of poly(ether carbonate)s 6 (PnNO$_2$, R = NO$_2$, n = 2–10; PnCN, R = CN, n = 6,10; PnBuO, R = BuO, n = 6,10; PnF, R = F, n = 6,10)

Polymers (PnNO$_2$, PnCN, PnBuO and PnF) were prepared by the experimental procedure used for PnNO$_2$ (n = 8), which is reported in detail as a typical example.

Polymerization reactions were carried out under nitrogen atmosphere in glass flasks equipped with Teflon stopcocks and rubber septa. Cationic catalyst BF_3·OEt_2 (1.6 μL, 0.013 mmol, 5 mol%) dissolved in methylene dichloride (0.5 mL) was introduced with a syringe into a nitrogen-purged reaction flask (5 mL) with a magnetic stirring bar, which contained the spiro-orthocarbonate monomer 4 (R = NO_2, n = 8) (0.20 g, 0.265 mmol) in methylene chloride (1.0 mL). The black-brown solution was stirred at room temperature for 72 h. The polymerization mixture was quenched by adding a few drops of triethylamine. The resulting brown transparent polymerization solution was diluted with methylene dichloride (1 mL) and was precipitated with methanol (100 mL). After removal of the solvent layer by decantation, the polymer was dissolved in methylene dichloride (0.3 mL) and the solution was added dropwise into vigorously stirred methanol (100 mL). This step was repeated twice more and the precipitated polymer was collected and dried in vacuum to yield 0.10 g (49.2%) of side-chain liquid-crystalline poly(ether carbonate) **6**, P8NO$_2$ (R = NO_2, n = 8), M_n = 3520, M_w/M_n = 1.55 by g.p.c.

^{1}H n.m.r. (δ, ppm, $CDCl_3$): 1.06–1.48 (br, 24H, $CH_2(CH_2)_6CH_2O$); 1.60–1.76 (br, 4H, $CHCH_2$); 1.76–2.06 (br, 2H, Hb); 3.16–3.42 (br, 4H, Ha); 3.82–3.95 (br, 2H, biphenyl–OCH_2); 3.95–4.22 (br, 4H, Hc); 6.83–8.24 (m, 16H, biphenyl protons). ^{13}C n.m.r. (δ, ppm, $CDCl_3$): 25.9, 26.9, 28.2, 29.1, 29.3, 29.6 (CH_2); 38.4 (Cb); 67.3 (Cc); 68.1 (ArO–CH_2); 70.8 (Ca); 115.4 (Cs); 124.0 (Cu'); 126.9 (Cs'); 128.4 (Cu); 130.7 (Ct); 146.9 (Ct'); 147.1 (Cr'); 155.3 (OC=O); 160.0 (Cr). I.r. (KBr, cm^{-1}): 1108 (s, νC–O–C); 1340 (s, $\nu_s NO_2$); 1512 (s, $\nu_{as} NO_2$); 1742 (s, νC=O).

RESULTS AND DISCUSSION

Synthesis and characterization

Ester exchange reaction of the biphenyl mesogenic 1,3-diols **3** with tetramethyl orthocarbonate in xylene according to the literature[15] afforded the spiro-orthocarbonate monomers **4**. The yields and h.r.m.s. data on **4** are presented in *Table 1*. The side-chain liquid-crystalline poly(ether carbonate)s **5** were synthesized by solution polymerization of the corresponding monomers following the published[16] procedures. The reaction pathway is considered to be similar to that proposed by Takata and Endo[17], as shown in *Scheme 2*. It is believed that successful overall transformation of spiro-orthocarbonate monomers **4** to the corresponding poly(ether carbonate)s **6** occurs via a single ring-opening isomerization process of cyclic trioxocarbonium ion-propagating intermediate [5]. G.p.c. analysis of the methanol-insoluble poly(ether carbonate)s showed that the number-average molecular weights (M_n) ranged from 2500 to 4300, with a unimodal distribution with polydispersity index (M_w/M_n) between 1.31 and 2.35. The results are presented in *Table 2*. *Figure 1a* depicts a representative ^{1}H n.m.r. spectrum of polymer P8NO$_2$. The polymer shows Ha and Hc protons at 3.16–3.42 and 3.95–4.22 ppm assignable to methylene protons adjacent to ether and oxocarbonyl linkages of the linear backbone, respectively. In the ^{13}C n.m.r. spectrum (*Figure 1c*) and DEPT subspectrum (*Figure 1b*, CH and CH_3 positive, CH_2 negative), methylene carbons of the main chain (Ca and Cc) were observed at 67.3 and 70.8 ppm. The signal of the monomer at 115.4 ppm, which is characteristic of ketal quaternary carbons of monomer M8NO$_2$, completely disappeared, and the signal assignable to carbonyl carbon appeared at 160.4 ppm. Furthermore, the carbonyl absorption at 1743 cm^{-1} due to the oxycarbonyl group is also confirmed in the i.r. spectrum. These data obviously suggest that spiro-orthocarbonate monomers **4** must have undergone quantitative double ring-opening to form the polymers **6** with ether carbonate repeating units, bearing biphenyl derivatives as the pendant anisometric cores.

Liquid-crystalline behaviour

The thermodynamic parameters of the phase transition and relevant phase assignments are summarized in *Table 1*, while *Figure 2* presents the d.s.c. curves of the representative monomers M6NO$_2$, M6CN, M6BuO, M6F and M10BuO. For monomers M6NO$_2$, M6CN, M6BuO and M6F containing six methylene spacers, two endothermic and exothermic peaks are observed in the heating and cooling cycles. For instance, the small peak at 111.2°C in the cooling scan of the monomer M6F, as shown in *Figure 2*, shows that the crystalline–nematic transition involves a small change of enthalpy (ΔH = 1.32 kcal mol^{-1}). On the other hand, the transition from nematic mesophase to the crystalline state results in a larger change in enthalpy (ΔH = 8.27 kcal mol^{-1}) at 86.8°C. The crystallization temperature also appears more supercooled in the cooling

Table 1 Yields, HR mass data, phase transitions and thermodynamic parameters of phase transitions for spiro-orthocarbonate monomers 3,9-*bis*[ω-(4'-R-biphenyloxy)alkyl]-1,5,7,11-tetraoxaspiro[5.5]undecanes

Monomer	R	n^a	Yield (%)	Molecular formula Exact mass (calc.)	$(m/z)^b$ (obs.)	Phase transitions and thermodynamic data[c]
$M2NO_2$	NO_2	2	40.0	$C_{35}H_{34}N_2O_{10}$ 642.2213	642.2219	K220.0(14.96)(15.27)I I195.5(0.18)(0.21)N158.6(10.63)(12.4)K
$M3NO_2$	NO_2	3	45.0	$C_{37}H_{38}N_2O_{10}$ 670.2526	670.2531	K196.7(7.36)(11.96)I I173.6(0.34)(0.38)N168.6(6.22)(7.09)K
$M4NO_2$	NO_2	4	68.4	$C_{39}H_{42}N_2O_{10}$ 698.2839	698.2829	K182.7(10.83)(11.96)I I164.4(0.75)(0.86)N140.0(7.72)(9.43)K
$M5NO_2$	NO_2	5	51.3	$C_{41}H_{46}N_2O_{10}$ 726.3152	726.3120	K188.1(14.67)(16.01)I I169.8(1.04)(1.18)N112.7(9.41)(12.27)K
$M6NO_2$	NO_2	6	59.5	$C_{43}H_{50}N_2O_{10}$ 754.3465	754.3463	K139.2(11.65)(14.22)N160.3(1.10)(1.27)I I159.7(1.15)(1.34)N108.6(10.50)(13.84)K
$M7NO_2$	NO_2	7	48.9	$C_{45}H_{54}N_2O_{10}$ 782.3778	782.3802	K141.0(10.14)(12.22)N154.6(1.16)(1.37)I I155.0(1.23)(1.52)N79.8(6.76)(9.64)K
$M8NO_2$	NO_2	8	47.1	$C_{47}H_{58}N_2O_{10}$ 810.4091	810.4954	K133.5(14.10)(17.46)N141.6(1.24)(1.51)I I139.1(1.29)(1.58)N91.7(11.59)(15.17)K
$M9NO_2$	NO_2	9	73.3	$C_{49}H_{62}N_2O_{10}$ 838.4404	838.4382	K128.0(14.39)(18.06)N144.8(1.52)(1.83)I I141.9(1.66)(2.01)N82.1(10.99)(15.58)K
$M10NO_2$	NO_2	10	64.0	$C_{51}H_{66}N_2O_{10}$ 866.4717	866.4712	K142.9(19.01)(23.00)I I135.9(1.69)(2.08)N105.0(15.14)(20.15)K
M6CN	CN	6	83.2	$C_{45}H_{50}N_2O_6$ 714.3669	714.3688	K175.5(12.96)(14.54)N181.8(2.29)(2.53)I I180.7(1.96)(2.17)N127.1(10.06)(12.65)K
M10CN	CN	10	64.0	$C_{53}H_{66}N_2O_6$ 826.4921	826.4891	K135.4(10.54)(12.99)N145.3(2.07)(2.49)I I142.2(2.51)(3.04)N92.0(6.85)(9.44)K
M6BuO	BuO	6	80.7	$C_{51}H_{68}O_8$ 808.4914	808.4894	K129.8S_x164.9(11.79)I I162.8(12.28)S_x100.5K
M10BuO	BuO	10	75.1	$C_{59}H_{84}O_8$ 920.6166	920.6172	K154.6(16.32)(19.21)I I149.0(16.00)(19.17)K
M6F	F	6	76.1	$C_{43}H_{50}O_6F_2$ 700.3575	700.3542	K111.5N120.5(8.69)(11.11)I I111.2(1.32)(1.73)N86.8(8.27)(11.57)K
M10F	F	10	76.2	$C_{51}H_{66}O_6F_2$ 812.4827	812.4930	K109.0(15.98)I I101.5(14.16)K

[a] Number of methylene carbons in the spacer
[b] By high-resolution mass spectrometry
[c] Phases: K, crystalline; N, nematic; S, smectic; I, isotropic. Numerical values in order quoted: transition temperature (°C) as determined by d.s.c. at 10°C min^{-1} in the first cooling and second heating runs and by microscopic observation; (corresponding enthalpy change (kcal mol^{-1})); (entropy change, $\Delta S/R$). Upper row, 2nd heating; lower row, 1st cooling

scan. *Figure 3a*, *b* and *c* show the typical nematic texture of $M6NO_2$, M6F and M6CN respectively. The small peak at 129.8°C in the d.s.c. scan for monomer M6BuO, shown in *Figure 2*, shows that the crystalline–smectic transition involves a small change in enthalpy, whereas the transition from the highly ordered smectic mesophase to the disordered isotropic state results in a larger change in enthalpy at 164.9°C. Monomer M6BuO exhibited a rod-shape texture, which is commonly associated with the smectic phase, as shown in *Figure 3d*. Only two monomers containing 10 methylene spacers—M10BuO and M10F—showed one endothermic and one exothermic peak in the heating and cooling cycles, respectively, as shown in *Figure 2*. These peaks were assigned to crystal-isotropic and isotropic-crystal transitions respectively, based on the results of optical microscopy. Therefore these monomers are not regarded as liquid crystalline.

The thermal transitions and thermodynamic parameters of polymers **6** are also listed in *Table 2*. *Figure 4* represents the d.s.c. curves of representative polymers $P6NO_2$, P6CN, P6BuO, P10BuO and P6F. As can be seen from *Table 2* and *Figure 4*, all polymers **6** exhibit liquid-crystalline behaviour and clearly showed glass transition temperatures (T_g). Polymer $P6NO_2$ showed glass transition temperatures at 25.2 and 21.9°C in the heating and cooling curves respectively. The thermodynamic parameter ΔH for the isotropization temperature of $P6NO_2$ was estimated to be 0.49 kcal per mole repeating unit (mru). In the cooling cycle, the same texture was also observed below 71.0°C, which was maintained unchanged down to room temperature.

The optical micrograph in *Figure 5a* confirms the LC behaviour of this polymer, showing a nematic schlieren texture. P6F did not exhibit the glass transition temperature in the d.s.c. cooling curve, as can be seen from *Figure 4*. In the heating part of the curve, though a prominent endothermic transiton (isotropization) was noted, with a relatively large enthalpy of isotropization (ΔH = 4.45 kcal mru^{-1}). In the cooling scan from the isotropic state, a spherulitic structure began to appear on the dark background at 85°C, growing gradually, and finally a mosaic texture was observed after prolonged annealing. No appreciable change was observed upon subsequent cooling to room temperature. A representative photomicrograph of the polymer P6F is shown in *Figure 5b*. Owing to the large enthalpy of isotropization and the mosaic texture observed by polarized optical microscopy, the phase of P6F is assumed to be a smectic mesophase. It has been reported that polyoxetane[7] and polybutadiene[18], containing the same fluorobiphenyl mesogenic group, also showed a smectic phase. The polymer P6BuO showed two endothermic peaks, associated with transitions between smectic mesophases at

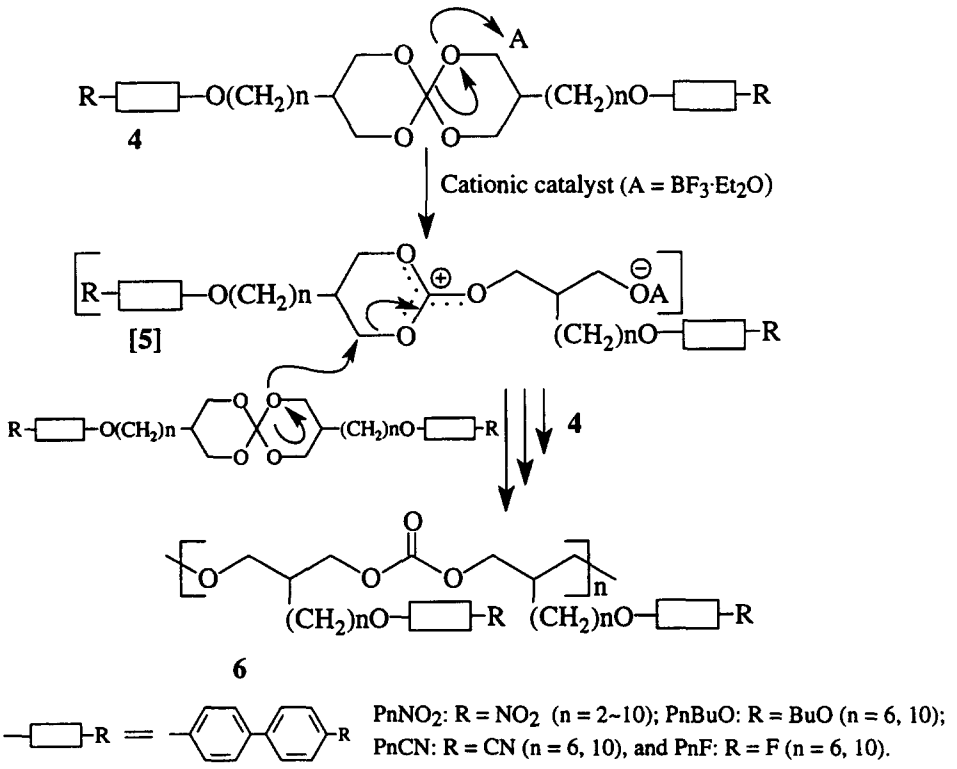

Scheme 2 Synthesis of side-chain liquid-crystalline poly(ether carbonate)s (P*n*NO_2, P*n*BuO, P*n*CN and P*n*F), **6**

Table 2 Cationic ring-opening polymerization[a] of spiro-orthocarbonate monomers having a biphenyl moiety at the side-chain end of poly(ether carbonate)s, and phase transitions and thermodynamic parameters

Polymer	R	n[b]	$[M]_0$[c] (10^{-2} mol L^{-1})	Yield (%)	M_n[d] (10^3)	MWD[d] (M_w/M_n)	Phase transitions and thermodynamic data[e]
P2NO_2	NO_2	2	3.8	65.1	2.52	1.44	G42.4N53.8(0.12)(0.11)I I47.8(0.14)(0.22)N34.4G
P3NO_2	NO_2	3	4.5	61.4	2.50	2.33	G44.3N132.9(0.11)(0.13)I I131.1(0.19)(0.24)N34.1G
P4NO_2	NO_2	4	11.1	58.5	2.87	2.35	G36.2N87.3(0.25)(0.34)I I82.8(0.25)(0.35)N31.3G
P5NO_2	NO_2	5	3.7	63.2	3.09	2.04	G25.6N88.1(0.36)(0.50)I I85.3(0.38)(0.49)N21.1G
P6NO_2	NO_2	6	17.8	52.6	3.70	1.35	G25.2N75.0(0.49)(0.71)I I71.0(0.47)(0.69)N21.9G
P7NO_2	NO_2	7	28.3	48.3	2.66	1.64	G22.9N99.4(0.78)(1.05)I I98.6(0.65)(0.88)N19.5G
P8NO_2	NO_2	8	17.6	49.2	3.52	1.55	G27.0N81.7(0.66)(0.94)I I78.7(0.77)(1.10)N18.2G
P9NO_2	NO_2	9	25.1	68.8	2.72	1.39	G21.9N115.6(4.60)(5.97)I I101.3(1.06)(1.43)N16.2G
P10NO_2	NO_2	10	14.0	58.2	3.32	2.12	G12.9S_A76.7(1.06)(1.52)I I77.4(1.32)(1.90)S_A9.0G
P6CN	CN	6	23.3	69.8	3.11	1.60	G26.1S_A92.4(0.19)(0.26)N101.1(0.72)(0.97)I I95.3(0.65)(0.89)N88.6(0.17)(0.24)S_A22.6G
P10CN	CN	10	16.5	74.2	3.80	1.38	G13.7S_A87.7(1.66)(2.32)I I86.2(1.60)(2.24)S_A10.1G
P6Bu0	BuO	6	10.5	77.1	3.11	1.31	G116.8S_E132.3(4.42)(5.49)S_A138.3(4.22)(5.16)I I136.7(3.44)(4.29)S_A127.8(5.85)(5.71)S_E106.8G
P10Bu0	BuO	10	3.2	69.8	4.30	1.34	G74.5S_E133.8(11.34)(14.00)I I130.9(3.45)(4.30)S_A129.0(5.85)(7.32)S_E70.5G
P6F	F	6	53.6	90.3	4.10	1.36	G52.0S_x87.0(4.45)(6.22)I I81.3(4.01)(5.69)S_x–G
P10F	F	10	24.6	83.1	3.80	1.48	G29.4S_x73.4(4.87)(7.08)I I65.9(4.36)(6.47)S_x26.0G

[a] In dichloromethane solvent at 25–30°C; initiator [I], BF_3–Et_2O; molar ratio [I]/$[M]_0 \approx 5\%$
[b] Number of methylene carbons in the spacer
[c] Initial concentration of charged monomer
[d] By g.p.c. in THF, correlated with standard polystyrene
[e] As footnote *c*, *Table 1*, except: G, glass; enthalpy change in kcal per mole repeating unit (mru)

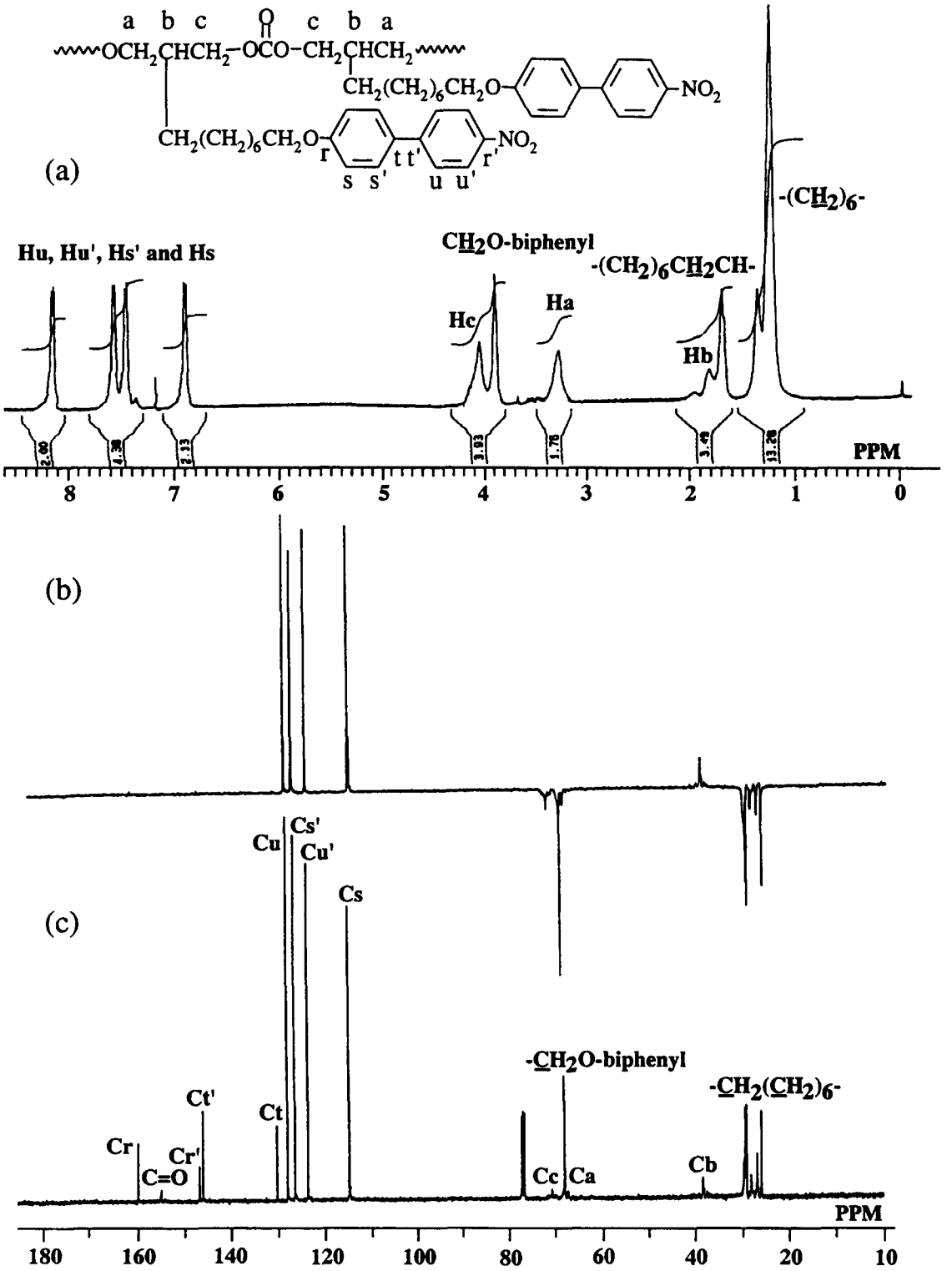

Figure 1 (a) ^{1}H n.m.r. spectrum, (c) ^{13}C n.m.r. spectrum and (b) DEPT subspectrum (400 MHz, δ, $CDCl_3$, Me_4Si) of the side-chain liquid crystalline poly(ether carbonate) $P8NO_2$

132.3°C and a smectic–isotropic transition (138.3°C). The glass transition temperature at 116.8°C was also detected as a weak but steep increase in heat capacity. The polymer P6BuO, containing a butoxy tail group, first displayed a typical focal conic texture, characteristic of a smectic A phase, during cooling from an isotropic phase, as observed by optical polarized microscopy. The temperature range for this biphasic region varied from 10 to 12°C. The transition to the second smectic mesophase was accompanied by the appearance of concentric rings in the area of conic fans[19]. This texture was classified as a paramorphotic fan-shape texture, associated with smectic E phase. Upon further cooling to room temperature and below, the fan texture with concentric rings was stable. The smectic A and smectic E characteristic textures as observed on cooling P6BuO are shown in *Figure 5c* and *d*. Similar thermal behaviour was also observed for polymer P10BuO, containing 10 methylene spacers. On the other hand, polymer P6CN exhibited an endothermic peak with one shoulder at 92.4°C, which was attributed to a smectic A–nematic transition, a

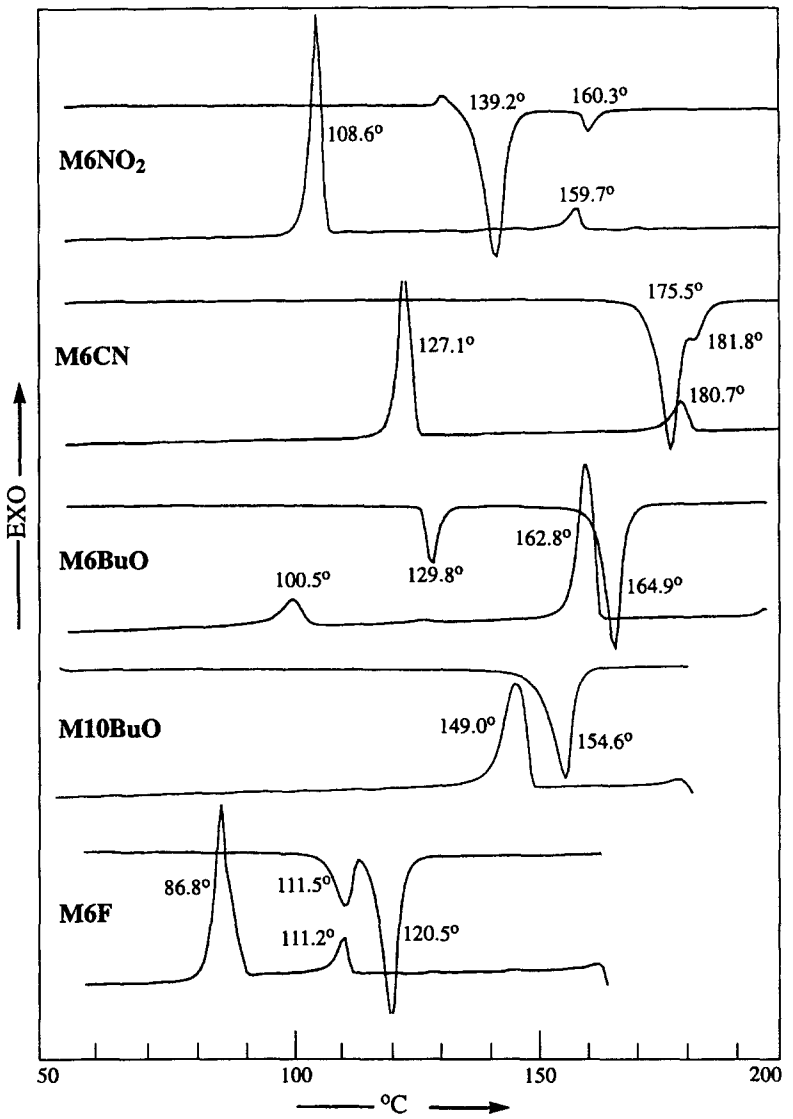

Figure 2 Heating and cooling d.s.c. traces of liquid-crystalline spiro-orthocarbonate monomer $M6NO_2$, M6CN, M6BuO, M10BuO and M6CN

higher-temperature endothermic peak at 101.1°C, which corresponded to a nematic–isotropic transition, and a glass transition temperature at 26.1°C, in the d.s.c. heating cycle. *Figure 5e* and *f* show the nematic texture and typical focal-conic smectic A texture respectively. All these transitions were reversible on cooling, and accordingly these polymers were classified as being enantiotropic in character. In contrast to the monomers M10BuO and M10F, which did not show the presence of any mesophase, polymers P10BuO and P10F were observed to be liquid-crystalline. Notably, all the polymers synthesized in this study containing 10 methylene spacers with nitro, butoxy, fluoro or cyano terminal groups showed smectic mesophases.

Richardt *et al.*[20] have reported that the length and polarity of the terminal groups on mesogenic moieties could strongly influence the mesomorphism and isotropic transition temperatures of side-chain liquid-crystalline polymers and low-molar-mass liquid crystals. In this study, three kinds of substituent, viz. NO_2, CN and F, were used. Results of the d.s.c. investigations of the series of monomers with six or ten methylene units with different tail groups are presented in *Figure 2*, clearly demonstrating the effects of substituents on phase behaviour and the transition temperatures, as given in *Table 1*. The d.s.c. first cooling curves in *Figure 2* show that the isotropic–mesophase temperature T_i of cyano-substituent monomer M6CN is higher than that of fluoro-substituted monomer M6F, and the transition temperature of nitro-substituted monomer $M6NO_2$ falls between the two. Of these monomers, M6CN exhibited the largest mesophase range (60.6°C), while its crystallization temperature T_c was higher than that of $M6NO_2$ and M6F. M6F had the lowest T_c (86.8°C), but its mesophase range was also found to be the smallest (24.4°C). These results reveal that the order of effectiveness of the terminal group in enhancing T_i is CN > NO_2 > F, which agrees well with the observations of Richardt *et al.*[20] and Attard *et al.*[21].

Let us again consider the side-chain liquid-crystalline poly(ether carbonate)s. The isotropic transition temperatures of the polymers with a six-carbon spacer are also highly dependent on the tail groups (terminal units). As illustrated in *Table 2* and *Figure 4*, the isotropic transition temperatures decrease for different tail groups in the order BuO > CN > F > NO_2. Although the nitro group is more polar than the fluoro group, an unexpected result—polymer $P6NO_2$ has a lower clearing temperature than P6F—has been observed in this study. It may be seen from *Figure 4* and *Table 2* that polymers P6F and $P6NO_2$ exhibit a T_i at 81.3 and 71.0°C respectively. As mentioned previously, P6F forms a smectic mesophase, whereas $P6NO_2$ shows a nematic mesophase. If we assume that the isotropic

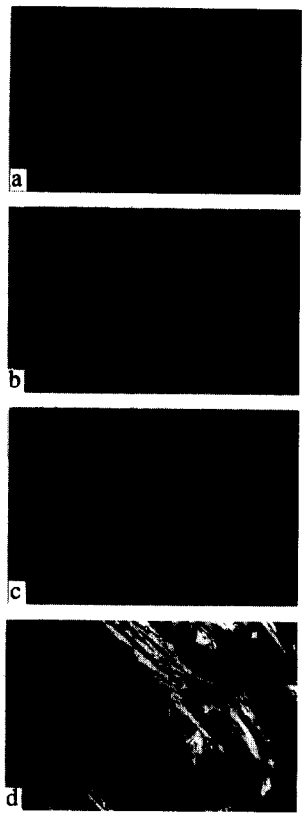

Figure 3 Optical polarization micrographs of monomers $M6NO_2$, M6F, M6CN and M6BuO: (a) N texture of $M6NO_2$ after cooling isotropic phase to 150.5°C; (b) N texture of M6F after cooling isotropic phase to 99.6°C; (c) N texture of M6CN after cooling isotropic phase to 170.2°C; (d) S_x texture of M6BuO after cooling isotropic phase to 150.0°C

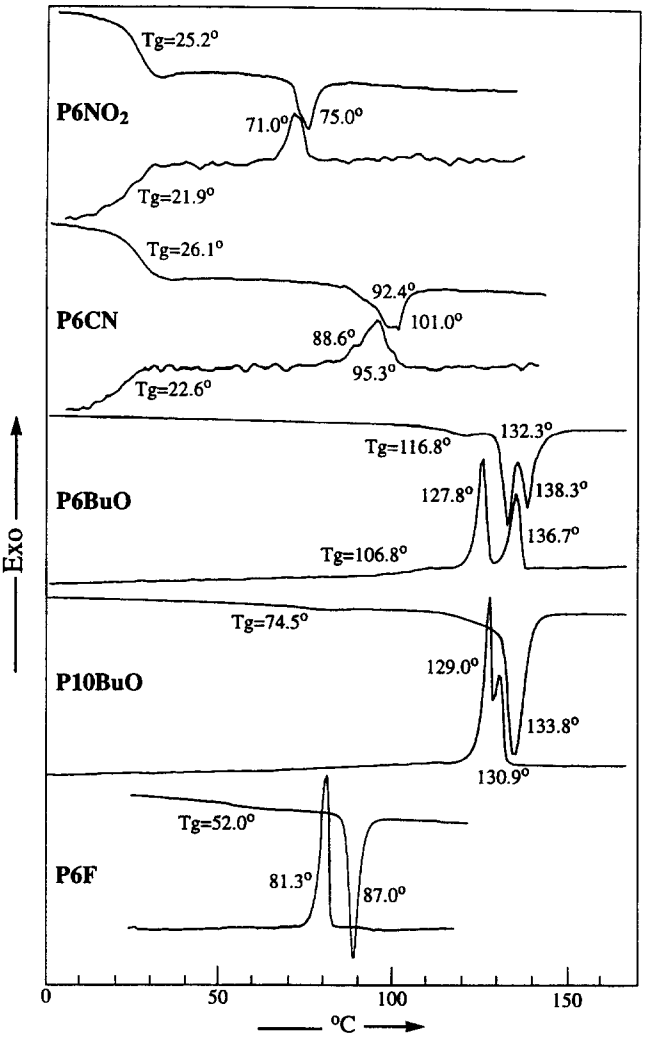

Figure 4 Heating and cooling d.s.c. traces of side-chain liquid-crystalline poly(ether carbonate)s $P6NO_2$, P6CN, P6BuO, P10BuO and P6CN

transition temperature is governed largely by the interaction of mesogenic cores, then the attractive forces between the polarizable electrons of the biphenyl rings apparently stabilize the more ordered smectic phase relative to the nematic phase. Therefore, P6F rightly exhibits a higher clearing temperature than $P6NO_2$. In contrast, the polymer $P10NO_2$ containing a 10-methylene spacer shows a higher isotropic transition temperature than the analogous polymer P10F containing fluoro-terminated side groups. $P10NO_2$ and P10F show a T_i at 77.4 and 65.9°C respectively, as given in *Table 2* (d.s.c. curves not shown). Since it has been observed that both $P10NO_2$ and P10F exhibit smectic mesophases, it may be concluded that similar packing exists between the biphenyl mesogenic cores. The origin of the extra stability of mesophase in polymer $P10NO_2$ can therefore be accounted for by considering the increased interaction of the mesogenic cores, resulting from the strong dipole of the nitro terminal group possessed by the biphenyl mesogenic group. Nevertheless, of the four poly(ether carbonate)s with equal spacer length (either six or ten methylene units), containing NO_2, CN, BuO and F tail groups, the polymers P6BuO and P10BuO, containing butoxy substituent, show the highest transition temperatures, 136.7 and 130.9°C respectively, as can be seen from the d.s.c. curves in *Figure 4* and *Table 2*. Apparently, a normal butoxy tail group adopts a favoured *trans* conformation in the liquid-crystalline phase, which leads to an enhanced aspect ratio of the mesogenic group. These results clearly demonstrate that both length and polarity of the terminal groups have a profound effect on the isotropic transition temperatures of

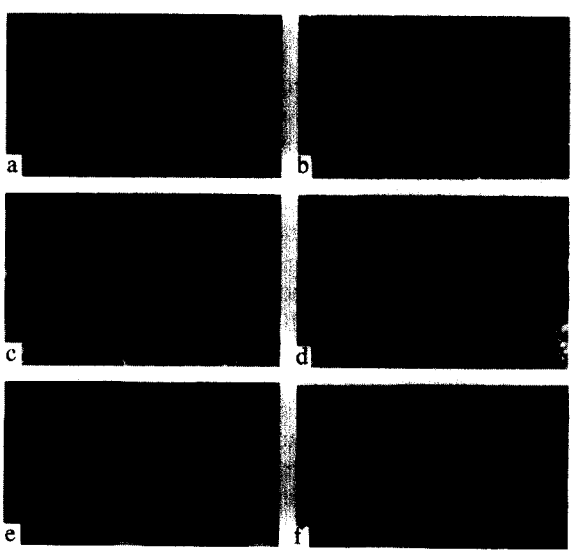

Figure 5 Optical polarization micrographs of polymers $P6NO_2$, P6F, P6BuO and P6CN: (a) N texture of $P6NO_2$ after cooling isotropic phase to 75.0°C; (b) smectic texture of P6F after cooling isotropic phase to 85.0°C and annealing for 36 h; (c) S_A texture of P6BuO after cooling isotropic phase to 135.0°C; (d) S_E texture of P6BuO after cooling isotropic phase to 125.0°C; (e) N texture of P6CN after cooling isotropic phase to 92.4°C; (f) S_A texture of P6CN after cooling isotropic phase to 71.6°C

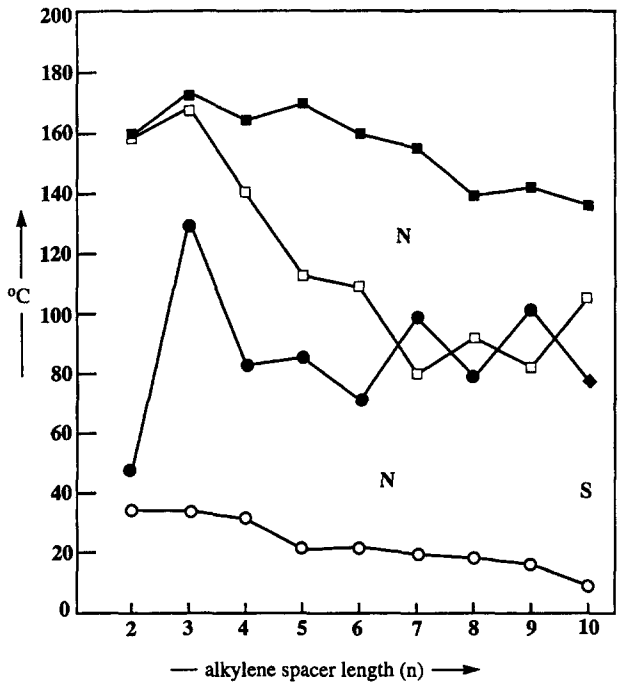

Figure 6 Dependence of transition temperatures on n, the number of methylene carbons in the spacer for the polymeric series PnNO$_2$: ○, glass transition; ●, nematic-isotropic transitions; ◆, smectic-isotropic transition. Also shown are the nematic-isotropic transitions (■) and the melting temperatures (□) for the monomeric series MnNO$_2$. Odd and even numbers of atoms in the spacer, including oxygen

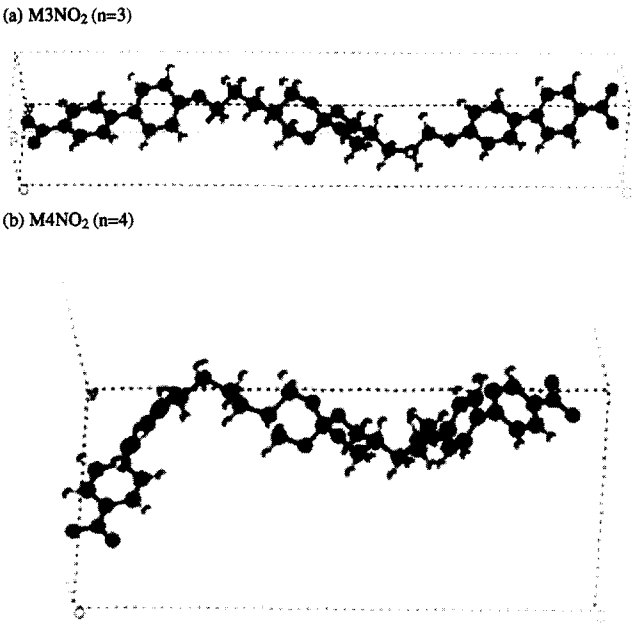

Figure 7 Computer-generated models of minimum energy conformations for (a) M3NO$_2$ (n = 3), even number of atoms in the spacer including oxygen atom, and (b) M4NO$_2$ (n = 4), odd number of atoms in the spacer including oxygen atom

spiro-orthocarbonate monomers **4** and side-chain liquid-crystalline poly(ether carbonate)s **6**.

The trends in glass transition and isotropization temperatures for the homologues of monomers MnNO$_2$ and polymers PnNO$_2$ (n = 2–10), as a function of the number n of methylene carbon atoms in the spacer, are presented in *Figure 6*. The glass transition temperature decreases slightly with increasing n, probably due to a plasticizing effect of the side chain on the backbone, in agreement with common findings for side-chain liquid-crystalline polymers. As can be clearly seen from *Figure 6*, the monomers **4**, MnNO$_2$, generally have far higher isotropization (or clearing) temperatures than those of the homologues of polymers **6**, PnNO$_2$. Imrie *et al.*[22] have also reported a similar thermal behaviour: the series of homologous side-chain liquid-crystalline poly{[4-[[α-[(4-nitrophenyl)azo]phenyl-4′-oxy]-ω-alkyl] oxy]styrene}s exhibited lower clearing temperatures than the analogous dimers, the α,ω-bis(4-nitroazobenzene-4′-oxy)alkanes. In the present study, the homologous series of spiro-orthocarbonate monomers **4** contained a flexible alkylene spacer bound at both the C-3 and C-9 positions of the six-membered spirocyclic ring to a biphenyl-based mesogenic rodlike molecular group. For brevity, these monomers can be considered as 'dimers'. Therefore, the enhanced transition temperatures of these 'dimers', compared with those of the corresponding polymers, can be attributed to the greatly increased molecular anisometry because of the presence of second mesogenic group. In addition, the transition temperature of the nitro homologues of the monomeric series MnNO$_2$ (n = 2–10) showed an odd–even effect of the carbon number of alkylene spacer, including the oxygen atom.

Figure 7 shows the calculated optimal structures of M3NO$_2$ and M4NO$_2$ (stick-and-ball model), obtained by using the software Cerius[2] of MSI (San Diego, USA) and Dreiding 2.21 force field[23], which were used to compute the energy and to minimize it by following 100 conformations of the Boltzmann jump method. The unit-cell dimensions, as estimated from these calculations, are a = 5.726, b = 5.712, c = 36.292 Å for M3NO$_2$ (*Figure 7a*), and a = 12.385, b = 14.630, c = 26.843 Å for M4NO$_2$ (*Figure 7b*). In comparison with the simulated molecular data, the volume of one unit cell occupied by M3NO$_2$ with even number of atoms in the spacer appears to be smaller than that for M4NO$_2$ with odd number of atoms in the spacer. Therefore, it can be concluded that the carbon number of the alkylene spacer contributes significantly to the molecular geometry of biphenyl-based spiro-orthocarbonate liquid-crystal monomers. As shown in *Figure 6*, for the nitro homologues of the monomeric series MnNO$_2$ (n = 2–10), the mesophase temperatures of the monomers with even number of atoms in the spacer (including the oxygen atom) are higher than those for monomers with odd number of atoms in the spacer. This may result from the fact that the 'even' molecule has a more elongated and rectlinear shape than the 'odd' molecule and is capable of packing with identical molecules in a more tightly parallel arrangement along any particular direction. *Figure 8* shows the trends in the isotropization entropies of the homologous monomers MnNO$_2$ and polymers PnNO$_2$ as a function of n. The isotropic transition entropies of both monomers and polymers increase with increasing number of methylene units in the flexible spacer, indicating an increasing contribution of the conformational freedom to the transition entropy associated with each transition.

CONCLUSIONS

Mesogenic spiro-orthcarbonate monomers containing six-membered spirocyclic rings are easily and conveniently prepared by condensation of the mesogenic 1,3-propanediols and tetramethyl orthocarbonate in xylene, using *p*-toluenesulfonic acid as catalyst. The

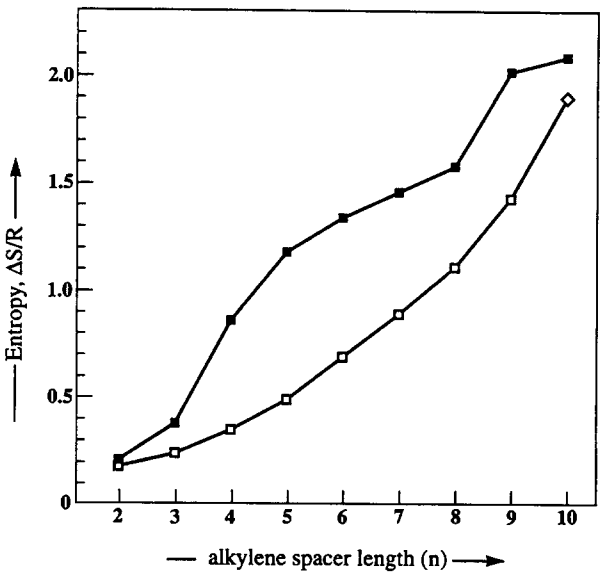

Figure 8 Dependence of isotropic entropies on number of alkylene spacers for the monomers M*n*NO_2 and polymers: ■, monomer nematic–isotropic transitions; □, polymer nematic–isotropic transitions; ◇, polymer smectic–isotropic transition

experimental results show that a novel poly(ether carbonate) can act as a main chain in side-chain liquid-crystalline polymers. The thermal properties of the polymers as well as the monomers are strongly affected by the length and polarity of the tail substituents on the mesogenic groups.

ACKNOWLEDGEMENTS

Financial support for this work from the National Science Council of the Republic of China, through grant no. NSC 81-0405-E-011-533, is gratefully acknowledged.

REFERENCES

1. (a) Finkelmann, H., Keichle, U. and Reharge, G., *Mol. Cryst. Liq. Cryst.*, 1983, **94**, 3453. (b) Kampf, I. G., *Ber. Bunsenges. Phys. Chem.*, 1985, **89**, 1179.
2. Rodriguez-Parada, J. M. and Percec, V., *J. Polym. Sci. A: Polym. Chem.*, 1987, **25**, 2269.
3. Fujishiro, K., Pajerski, A. D. and Lenz, R. W., *Liq. Cryst.*, 1992, **12**, 417, 561.
4. Tuan, P. A., Kostromin, S. G. and Shibaev, V. P., *Polymer Bulletin*, 1992, **29**, 49.
5. Bonnans-Plaisance, C., Levesque, G. and Pomepui, B., *Polymer*, 1993, **34**, 2003.
6. Kawakami, Y. and Takahashi, K., *Polymer Bulletin*, 1991, **25**, 521.
7. Kawakami, Y., Takahashi, K. and Hibino, H., *Macromolecules*, 1991, **24**, 4531.
8. Kawakami, Y., Takahashi, K., Nishiguchi, S. and Toida, K., *Polymer International*, 1993, **31**, 35.
9. Sargeant, S. J. and Weber, W. P., *Polymer Preprint*, 1993, **34**(1), 290.
10. (a) Komiya, Z., Pugh, C. and Shrock, R. R., *Macromolecules*, 1992, **25**, 6586. (b) Pugh, C. and Arehart, S. V., *Polymer Preprint*, 1996, **37**(1), 72.
11. LesLie, T. M., Demartino, R. N., Choe, E. W., Khanarian, G., Struetz, D. E., Tang, C. C. and Yoon, H. N., *Mol. Cryst. Liq. Cryst.*, 1987, **153**, 451.
12. (a) Vogel, A. I., *Textbook of Practical Organic Chemistry*, 5th edn. Longman, London, 1989, p. 939. (b) Bellamy, F. D., *Tetrahedron Letters*, 1984, **25**, 839.
13. Percec, V., Rodriguez, J. M. and Polym, J., *J. Polym. Sci. A: Polym. Chem.*, 1986, **24**, 1363.
14. McRoberts, A. M., Denman, R. and Gray, G. W., *Macromol. Chem. Rapid Commun.*, 1990, **11**, 617.
15. Endo, T. and Okawara, M., *Synthesis*, 1984, 837.
16. Endo, T., Sato, H. and Takata, T., *Macromolecules*, 1987, **20**, 1416.
17. Takata, T. and Endo, T., *Macromolecules*, 1988, **21**, 900.
18. Kawakami, Y., Toida, K. and Ito, Y., *Macromolecules*, 1993, **26**, 1177.
19. Gray, G. W. and Goodby, J. W. G., *Smectic Liquid Crystals—Texture and Structures*. Leonard Hill, London, 1984.
20. Richardt, H., Mauzac, M., Nguyea, H. T., Sigaud, G., Achard, M. F., Hardouin, F. and Gasparoux, H., *Mol. Cryst. Liq. Cryst.*, 1988, **155**, 141.
21. Attard, G. S., Dave, J. S. and Wallington, A., *Makromol. Chem.*, 1991, **192**, 1495.
22. Imrie, C. T., Karasz, F. E. and Attard, G. S., *Macromolecules*, 1993, **26**, 545.
23. Mayo, S. L., Olafson, B. D. and Godland, W. A. III, *J. Phys. Chem.*, 1990, **94**, 8897.